An InP-based integrated modulated coherent state source for differential phase shift quantum key distribution

H. O. Çirkinoglu,[1] R. Santos[2], K.Williams[1], and X. Leijtens[1]

[1]Eindhoven University of Technology, 5612 AZ, Eindhoven, The Netherlands
[2] SMART Photonics, Eindhoven, The Netherlands

A low-cost integrated differential phase shift QKD transmitter, which consist of a distributed Bragg reflector laser, a phase modulator, and Mach-Zehnder modulator sections for pulse carving and optical attenuation is presented. Initial characterization results of the laser, and the modulator sections are demonstrated.

Introduction

Quantum communication offers theoretically secure sharing of information through exploitation of the probabilistic nature of quantum physics [1]. Secure sharing of encryption keys can be guaranteed through quantum key distribution (QKD), without making any assumptions on how much computational power an eavesdropper might have [2]. Even though many successful quantum key distribution applications have been demonstrated [3, 4], many of them rely on expensive and hard-to-control bulk optics. Integrated photonic circuits offer scalable, low cost and robust realizations of quantum key distribution, allowing the technology to be accessible publicly, and for larger scale applications [5, 6]. Over more than three decades, there have been a number of discrete-variable protocols described for quantum key distribution including BB84 [7], differential-phase shift (DPS) [8], and coherent-one-way (COW) [9]. In this work, we present a weak coherent state source to serve as a DPS QKD transmitter, fabricated using the generic platform of Smart Photonics [10, 11], as a part of the European Quantum Flagship project UNIQORN [12]. The fabricated transmitter consists of a distributed Bragg reflector (DBR) laser, an electro-refraction modulator to control the phase between pulses, a Mach-Zehnder Pulse carver to erase transition effects, and variable optical attenuator (VOA) stages to achieve the required signal levels. The security of the quantum channel is potentially compromised by the imperfect modulation of amplitude and phase of the transmitted signal [13]. We report on the initial characterizations of the components of the chip. We analyze the transmitter in terms of its linewidth, which is affecting the stability of the phase of the pulse, as well as the extinction ratio of the pulse carver, and the characteristics of the variable optical attenuator, all of which play important roles in the control of the average number of photons transmitted per pulse.

Differential phase shift quantum key distribution

In DPS QKD using coherent light [14], the sender Alice prepares a pulse train of weak coherent states with average photon number of less than one, where the phase of each state is encoded randomly between $\{0, \pi\}$. The receiver Bob divides the received signal into two paths, and recombines them using a delay interferometer (DI) with a delay time equal to the time between each consecutive pulses. The DI is followed by photon detectors at its two outputs. The phase information at a time instance is retrieved based on which detector detects a photon. After transmission and detection, Bob reveals the information of the time instances at which a photon is detected. From this information, Alice can

deduce what bit string Bob has. Compared to the well-known BB84 protocol, DPS QKD is advantageous due to the simplicity of detection, and utilization of each detected photon without the need of basis choice or sifting [15].

Transmitter Chip

The realized transmitter employs a light source consisting of a DBR laser [16] for light generation, an electro-refractive phase modulator section for phase encoding of the signal, and a Mach-Zehnder modulator with electro-refractive modulators (ERM) in each of the interferometer arms for pulse carving. Multimode interference devices are used for splitting and combining of the signals. The transmitter is designed to be capable of switching between the classical and the quantum signal regime. In order to attain the required signal attenuation, the source is followed by a variable optical attenuator (VOA) function. For this, the circuit employs a cascade of three tunable Mach-Zehnder interferometers that can be tuned to each achieve up to 20 dB suppression. A schematic of the circuit, and a microscope image of the chip is shown in figure 1. The fabricated devices are being characterized and first results of the static characterization are presented below.

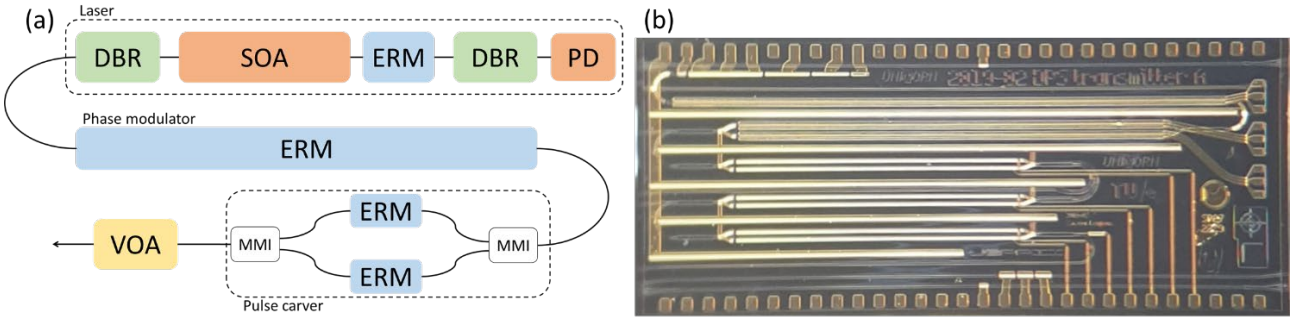

Figure 1 - (a) The schematic of the DPS QKD transmitter chip, (b) Microscope image of the fabricated chip

The DBR laser operates as expected. The LIV characteristics of the laser is depicted in figure 2(a), where the output light power is monitored using the photodiode on the laser structure, which typically has a responsivity of 0.8 A/W. At 22.1 ºC, the laser exhibits a threshold current of 28 mA. The linear operation of the laser indicates an optical power on the order of a few milliwatts at the maximum drive current of 100 mA.

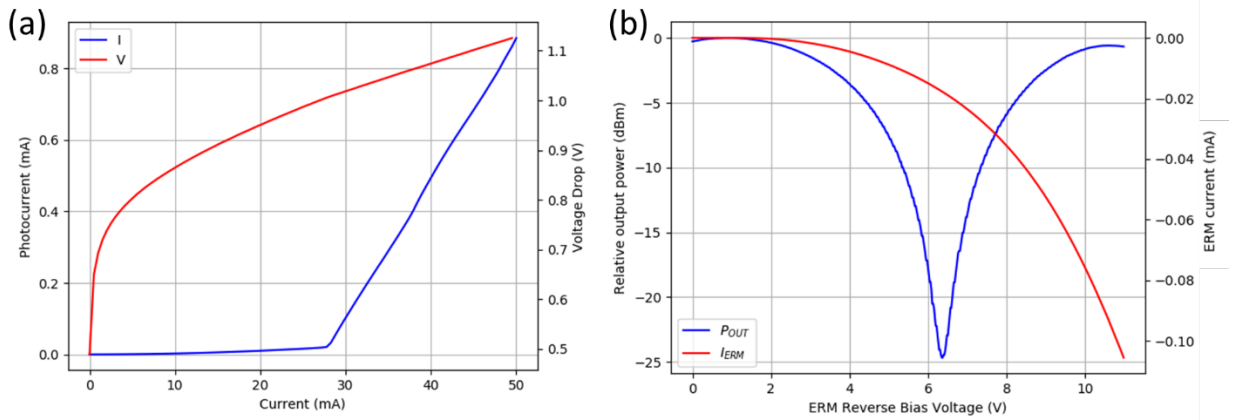

Figure 2 – (a) LIV characteristics of the DBR laser, (b) The relative transmission of the first stage attenuator based on electro-refraction.

The attenuation of the output signal with the Mach-Zehnder-based VOA is evaluated. The output optical power, and the photo-current generated in the 2-mm-long active modulator section is recorded while varying the applied reverse bias voltage to one of the arms of the interferometer. The second arm is kept at a constant bias voltage. The response is given in figure 2(b). The figure shows a good extinction ratio of 24.6 dB, and a bias voltage of -5.4 V is needed for π phase shift. The additional attenuation, introduced due to the absorption by the ERM section is at a level of 0.6 dB at 9.7 V bias voltage.

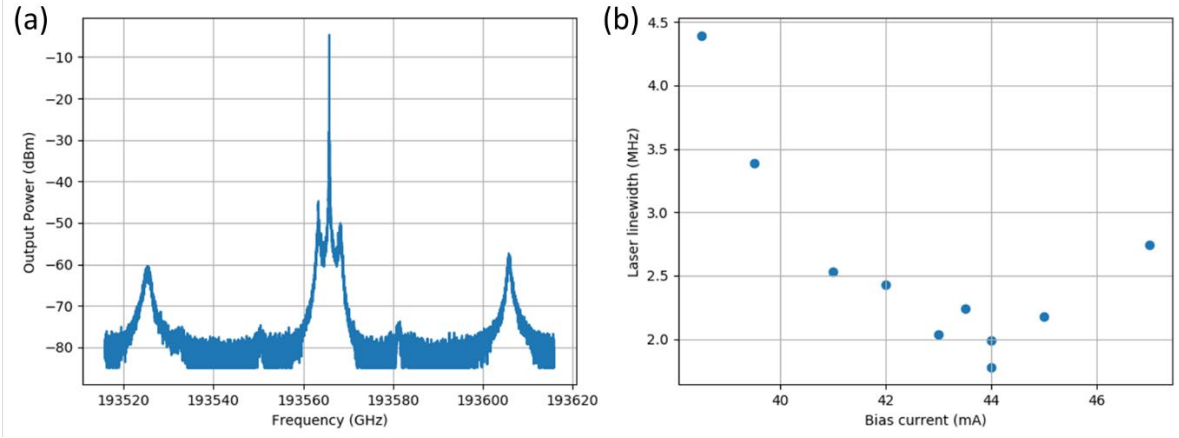

Figure 3 – (a) Optical spectrum of the DBR laser (b) Linewidth measurement results for different bias current values

The optical spectrum, recorded by APEX 2041A spectrum analyzer with a resolution of 20 MHz is depicted in figure 3(a). The laser operating at 44 mA drive current results in a single mode emission around 1550 nm with >55 dB side-mode-suppression ratio. Two neighboring peaks around the main mode result from a relaxation oscillation frequency of around 3 GHz. The linewidth measurements for various bias current values are acquired using OEWaves OE4000 phase noise and linewidth measurement system, and are given in figure 3(b). The measurements display a laser linewidth of ~2MHz around 44 mA bias current. For 1 GHz modulation of the signal, a linewidth of 2 MHz corresponds to 0.2% of the receiver interferometer free-spectral-range, which results in a quantum bit error rate of <0.5% [13].

Discussion

The tests carried out so far indicate proper functioning of the tested components. The bit rate of quantum key distribution depends directly on the achievable modulation speed of the signal. In our case, we aim to reach 10 GHz modulation using electro-refraction modulators. Considering recent results obtained for electro-refraction modulators that are fabricated in the same process and with proper electrode design [17], our target is within the technological capabilities. We plan to further inspect the dynamic response of the ERM structures which are used for phase modulation, and pulse carving. For performing the dynamic measurements, the samples need to be wire-bonded and connectorized, in order to drive all required signals simultaneously.

Based on our measurements, we expect to be able to attenuate the signal by > 60 dB, with a three-stage VOA. Generation of weak coherent states requires attenuation of the optical signal to a level of <1 photons per pulse, while maintaining a good optical signal-to-noise ratio. In our device, where the light source is integrated together with rest of the circuit,

the signal suffers from a broadband noise, which originates from spontaneous emission at the laser active region. The part of this noise that is guided through the waveguide structures is also attenuated by the VOA sections, while being attenuated not as efficiently as the signal due to its broadband nature. Furthermore, the unguided stray noise in the circuit remains independent from the applied attenuation, decreasing the signal-to noise ratio as signal power is reduced. We plan to further investigate the change in the SNR as a function of the applied attenuation.

Acknowledgements

This work has received funding from the European Union's Horizon 2020 research and innovation programme through the Quantum-Flagship project UNIQORN under grant agreement No 820474. Nazca Design was used to generate the mask layout in this work.

References

[1] H.K. Lo, M. Curty, and K. Tamaki, "Secure quantum key distribution," Nature Photonics, vol. 8, 595-604, 2014.
[2] V. Scarani, H. Bechmann-Pasquinucci, N.J. Cerf, M. Dušek, N. Lütkenhaus, and M. Peev, "The security of practical quantum key distribution," Reviews of Modern Physics, vol. 81, 1301-1350, 2009.
[3] H. Takesue, E. Diamanti, T. Honjo, C. Langrock, M.M. Fejer, K. Inoue, and Y. Yamamoto, "Differential phase shift quantum key distribution experiment over 105 km fibre," New Journal of Physics, vol. 7, 232, 2005.
[4] M. B. Costa e Silva, Q. Xu, S. Agnolini, P. Gallion, and F.J. Mendieta. "Homodyne detection for quantum key distribution: an alternative to photon counting in BB84 protocol" in Proceedings of SPIE Photonics North, vol. 6343, 63431R, 2006.
[5] P. Sibson, C. Erven, M. Godfrey, S. Miki, T. Yamashita, M. Fujiwara, M. Sasaki, H. Terai, M.G. Tanner, C.M. Natarajan, R.H. Hadfield, J.L. O'Brien, and M.G. Thompson, "Chip-based quantum key distribution," Nature Communications, vol. 8, 13984, 2017.
[6] P. Sibson, J.E. Kennard, S. Stanisic, C. Erven, J.L. O'Brian, and M.G. Thompson, "Integrated silicon photonics for high-speed quantum key distribution," Optica, vol. 4, 172-177, 2017.
[7] C.H. Bennett, and G. Brassard, "Quantum public key distribution system," IBM Technical Disclosure Bulletin, vol. 28, 3153-3163, 1985.
[8] K. Inoue, E. Waks, and Y. Yamamoto, "Differential phase shift quantum key distribution," Physical Review Letters, vol. 89, 037902, 2002.
[9] D. Stucki, N. Brunner, N. Gisin, V. Scarani, and H. Zbinden, "Fast and simple one-way quantum key distribution," Applied Physics Letters, vol. 87, 194108, 2005.
[10] Smit, Meint, et al, "An introduction to InP-based generic integration technology," Semiconductor Science and Technology, vol. 29.8, 083001, 2014.
[11] "Smart Photonics", http://smartphotonics.nl.
[12] "UNIQORN Project", http://quantum-uniqorn.eu.
[13] T. Honjo, T. Inoue, and K. Inoue, "Influence of light source linewidth in differential-phase-shift quantum key distribution systems," Optics Communications, vol. 284, 5856-5859, 2011.
[14] K. Inoue, E. Waks, and Y. Yamamoto. "Differential-phase-shift quantum key distribution using coherent light." Physical Review A vol. 68.2, 022317, 2003.
[15] B. Schrenk, M. Hentschel, and H. Hübel. "Single-Laser Differential Phase Shift Transmitter for Small Form-Factor Quantum Key Distribution Optics." Optical Fiber Communications Conference and Exposition (OFC), IEEE, 1-3, 2018.
[16] D. Zhao, "High-precision Distributed Bragg Reflectors in a Generic Photonics Integration Platform". PhD thesis, Eindhoven University of Technology, Eindhoven, The Netherlands, 2018. ISBN 978-90-386-4627-5.
[17] W. Yao, B. Smalbrugge, M. K. Smit, K. A. Williams, and M. J. Wale. "A 6× 30 Gb/s Tunable Transmitter PIC With Low RF Crosstalk From an Open-Access InP Foundry." IEEE Journal of Selected Topics in Quantum Electronics, vol. 25, no. 5, 1-10, 2019.